35th Annual International Conference of the IEEE EMBS
Osaka, Japan, 3 - 7 July, 2013

Hemodynamics at the Ostium of Cerebral Aneurysms with Relation to Post-Treatment Changes by a Virtual Flow Diverter: A Computational Fluid Dynamics Study*

Christof Karmonik, *Member, IEEE*, Gouthami Chintalapani, Thomas Redel, Y Jonathan Zhang, Orlando Diaz, Richard Klucznik, Robert G Grossman

Abstract— **Computational fluid dynamics (CFD) techniques have been refined for modeling the hemodynamics in cerebral aneurysms. Recent interest has focused on understanding hemodynamic changes by treatment with a flow diverter (FD), i.e. a stent with a dense metal mesh which is placed across the ostium to divert the majority of flow away from the aneurysm. Potential complications include remnant inflow jets but, more seriously, aneurysm hemorrhage. For optimization of treatment outcome, a better understanding of the effects caused by the FD would be beneficial. In particular, pressure and velocity distributions at the aneurysm ostium are of interest, as they will be directly affected by the FD which in turn will influence post-treatment hemodynamics inside the aneurysm. Here, we report the results of a CFD study investigating the relationship between pre-treatment and post-treatment velocities, pressures and wall shear stresses (WSS) in the aneurysm with corresponding hemodynamic conditions at the aneurysm ostium prior to treatment. The study was carried out using a dedicated CFD prototype which allows modeling the effects of a virtual FD integrated into patient-specific geometries utilizing Darcy's law. Velocities and WSS were reduced in all cases post FD treatment, pressure increased in one case. Heterogeneous distributions of the velocity magnitude were found at the ostium with focal maxima indicating potential risk zones for remnant inflow jets into the aneurysms. Pressures at the ostium correlated with pressure changes inside the aneurysm which could become a pre-treatment indicator for the evaluation of the suitability of a particular aneurysm for FD treatment.**

I. Introduction

Recently, a new endovascular technique was developed, in which a stent with a dense mesh (flow diverter, FD) is placed across the ostium with the intent to divert blood flow away from the aneurysm thereby introducing blood coagulation inside the aneurysmal sac. FD treatment is indicated for a subgroup of aneurysms, such as complex aneurysms (fusiform, large and giant, wide neck small aneurysms) which are considered untreatable by the conventional endovascular approach (coiling). In addition, recurrences of a previously coiled aneurysm may be treated by FD [1]. Clinical reports mainly of single center experiences have demonstrated successful application of this technique [2, 3] and larger trials are currently preformed to assess its efficacy [4].At the same time, serious adverse outcomes have been reported such as death by early or late fatal hemorrhage from aneurysm rupture or from acute thrombosis [5, 6].

Computational fluid dynamics (CFD) techniques, initially developed to identify additional risk factors for aneurysm rupture [7-9]. have also been employed to investigate hemodynamics after FD treatment [10]. That study investigated 3 aneurysms which ruptured after FD treatment and 4 which did not. Ruptured aneurysms showed increased pressure in the aneurysmal sac post-treatment despite successful flow diversion. A better understanding of post-treatment hemodynamic changes and how these correlate with observed hemodynamic parameters prior to treatment may therefore be beneficial for evaluating a particular aneurysm for FD treatment. Of particular interest are post-treatment pressure increases, as these may eventually lead to aneurysm rupture with potentially fatal outcome.

Here we present a study where the hemodynamics in eight intracranial aneurysms of the internal carotid artery (ICA) were simulated, which were treated with FD in our institution. Using CFD, velocities, pressures and wall shear stresses (WSS) before and after placement of a virtual FD into a computational model designed from patient-specific image data were derived.

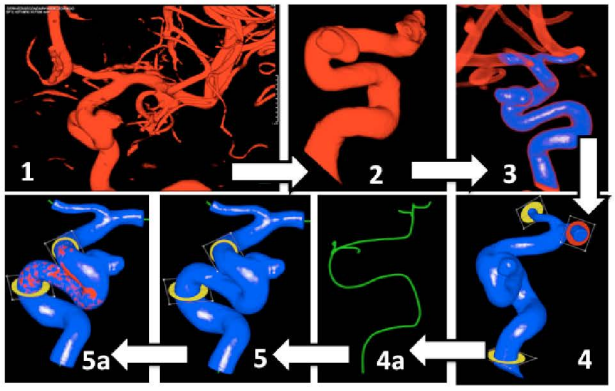

Figure 1: From 3D DSA data to computational mesh using the workflow implemented in the CFD Research Prototype (Siemens AG). Numbers refer to steps explained in the text. In addition, panel 4a shows centerline across the aneurysm and panel 5a the virtual FD in red overlaid onto the blue aneurysm model.

*Support by Siemens AG is gratefully acknowledged..

C. Karmonik, YJ Zhang and RG Grossman are with the Department of Neurosurgery, O Diaz and R Klucznik with the Department of Radiology, The Methodist Hospital, Houston TX 77030, USA (phone: 713-441-3800; fax: 713-793-1004; e-mail: ckarmonik@ tmhs.org).

G Chintalapani is with Siemens Medical Solutions USA INC, Hoffman Estates, IL

T. Redel is with Siemens AG, Forchheim, Germany

The study was conducted with a CFD Research Prototype (Siemens AG) with the capability of simulating the effects of a FD by modeling it as a porous medium. Hemodynamics at the aneurysm ostium and inside the aneurysmal sac prior to treatment were quantified and compared to hemodynamics post-treatment.

II. Materials and Methods

A. CFD Simulations

IRB approval was obtained for this study. 3D digital angiography subtraction (DSA) image data was retrospectively collected for eight ICA aneurysms. Image data was transferred to the dedicated workstation of the CFD Research Prototype (Siemens AG).

TABLE I. Aneurysm size and Surface Mesh Information

case	*size (diameter) [mm]*	*Number of vertices of STL surface mesh*	*Number of Faces of STL surface mesh*
1	6.6	98,528	197,052
2	9.5	135,469	270,936
3	5.2	12,448	24,892
4	7.5	75,087	150,174
5	8.2	32,056	64,108
6	2.1	65,973	131,942
7	6.4	138,191	276,382
8	2.8	28,074	56,144

Computational models were created by completing the separate steps of a predefined workflow (Figure 1). In step 1, the anonymized 3D DSA images (DICOM format) after export from a clinical workstation were directly imported into the CFD Prototype research workstation and a 3D surface model of the corresponding vasculature was created. In step 2, a 3D cropping interface was then employed to define the region of interest, to remove small arterial branches and to eliminate venous contamination (if present). In step 3, the surface of the 3D computational model was segmented using region-growing and thresholding algorithms. In step 4, by clicking on derived centerlines, inflow and outflow regions were specified at appropriate locations. In step 5, the centerlines were also used to define the proximal and distal locations of the virtual FD. CFD simulations were performed with and without FD using the same inflow condition in all cases (maximum inflow velocity 0.8 m/s). The CFD Research Prototype (Siemens AG) uses a level-set based embedded boundary method for the solution of the Navier-Stokes equations with the use-specified boundary conditions [11]. Blood was modeled as an incompressible fluid with a density of 1000 kg/m^3 and a viscosity of 0.004 kg/ms). The FD was modeled as a porous interface embedded in the flow domain [12], with the following parameters: hydraulic resistance (tangential: 1,700 mm^{-2}, normal: 890 mm^{-2}) and viscous resistance (tangential: 4.7 mm^{-1}, normal: 8.7 mm^{-1}).

Simulation results were stored on disk using the visualization toolkit (vtk) file format (Kitware Inc.). In addition, the surface mesh and the FD mesh were stored on disk in the stereolithographic (STL) file format. In total, eight ICA aneurysms were simulated (aneurysm size and size information for the computational mesh, see table 1).

B Analysis of Simulation Results

Simulation results (in vtk format) and FD mesh (in STL format) were imported into Paraview (Kitware, Inc.).

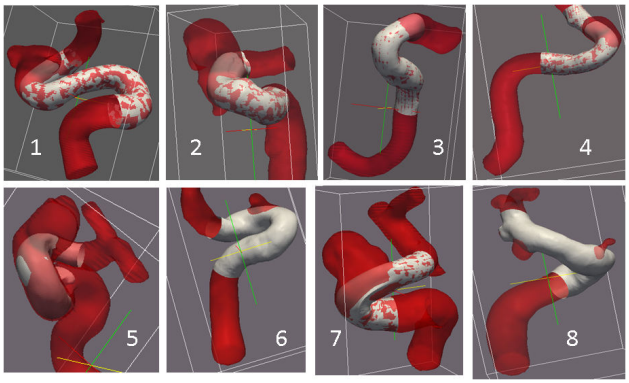

Figure 2: Computational models of aneurysms (red) with virtual FD meshes (gray).

Velocities, pressures and WSS values inside the aneurysm and on the aneurysm wall were segmented using the Paraview 3D segmentation tool and stored in a comma-separated values (csv) file. Using the FD mesh and the simulation results obtained without FD, velocities and pressures at the aneurysm ostium were visualized (Figure 3) and stored in a csv file by employing the 'Resample with Dataset' filter in Paraview. The csv files were analyzed by scripts written in the R statistical language.

Mean values were calculated for the following hemodynamic parameters: 1) blood velocity inside the aneurysm pre-treatment, 2) pressure inside the aneurysm pre-treatment va1, 3) WSS on the aneurysm wall pre-treatment WSSa1, 4) blood velocity at the aneurysm ostium pre-treatment vo, 5) pressure at the aneurysm ostium pre-treatment po, 6) blood velocity inside the aneurysm post-treatment va2, 7) pressure inside the aneurysm post-treatment pa2, 8) WSS on the aneurysm wall post-treatment WSSa2 and 9) pressure change (post-pre) inside the aneurysm Δpa. A correlation matrix was established for these quantities (Pearson correlation coefficient (cc)) and data with high correlation (cc> 0.7) were further investigated. Correlation of the hemodynamic parameters introduced above (1-9) with aneurysm size (Sa) was also investigated.

III. Results

A. Pre-Processing

Image data processing took less than 45 min in all cases. The ability to directly use the clinical image data without the need of format conversion and the 3D cropping interface greatly facilitated this process. Approximating the behavior of a real FD, the virtual FD created by the prototype software

was in all cases similar in diameter to the parent artery. As a consequence, due to the mismatch of the cylindrical shape of the virtual FD with the enlarged parent artery segment across the aneurysm, this resulted in a large aneurysm ostium area for the wide-neck aneurysm cases (1,2,3,5 and 7) (as can be seen in Figure 2).

B. Hemodynamic Parameters

Velocities and WSS decreased in all cases, pressure increased in one (case 1, Figure 3a and b) indicating a successful diversion of flow with variable of pressure changes.

At the ostium, the distribution of velocities (Figure 4) was more variable than the ones for the pressure (Figure 4) exhibiting distinct focal maxima and minima corresponding to inflow and outflow zones. This pattern was found in both the large-neck as well as the small-neck aneurysms. Average velocities inside the aneurysm ranged from 7 % (case 6) to

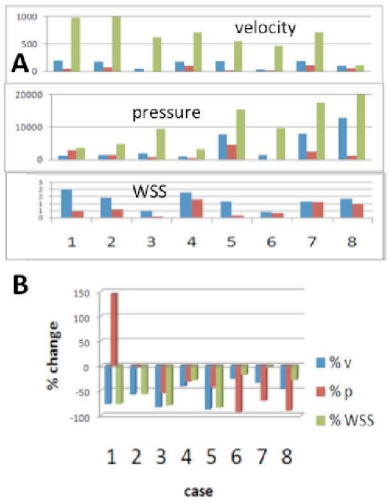

Figure 3: A Hemodynamic parameters pre (blue) and post (red) compared to values at the ostium (green). **B**: % change of velocity (v), pressure (p) and WSS for each aneurysm.

93 % (case 8) of the ones found at the ostium prior to virtual FD placement whereas pressures ranged from 15 % (case 6) to 51 % (case 5) (Figure 3a).

C. Correlation of Hemodynamic Parameters

From all investigated correlations, only 9 had absolute values larger than 0.70 ($p<0.05$):

1) va1 and WSSa1: cc=0.80,p=0.01,
2) va1 and pa2: cc=0.71, p=0.03,
3) va2 and pa2: cc=0.90, p=0.001,
4) pa1 and po: cc=0.89, p=0.001,
5) Δpa and pa1: cc=-0.95,p=0.0001,
6) Δpa and po: cc=-0.95,p=0.0001,
7) pa1 and vo: cc=-0.68,p=0.03,
8) vo and po: cc=-0.80,p=0.01
9) Δpa and vo: cc=0.79,p=0.01

Of those, 1), 3), 4), 7) and 8) express expected relations between physical quantities. Of particular interest are findings 6) and 9) which relate the velocities and pressures at the aneurysm ostium *before* treatment with the pressure changes in the aneurysm *after* virtual FD treatment (Figure 5). No statistically significant correlations of any hemodynamic parameters with aneurysm size (Sa) were found.

IV. Discussion

The application of CFD techniques as described here is an

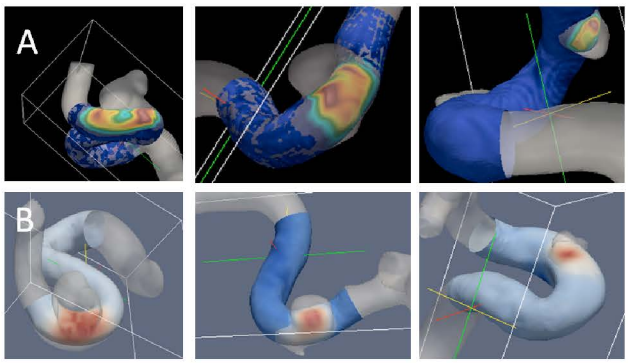

Figure 4: A: Velocity and **B**: pressure distribution at the ostium for a large (left), medium (center) and small (right) neck aneurysm (red color denotes high values, blue color low values).

example of the concept of virtual surgery, where an intervention is first simulated or virtually performed to obtain a better understanding of its impact. The design of the CFD prototype favors such an application: patient-specific image data can be imported directly into the software without a format conversion thereby reducing time, user interaction and a potential source of error (i.e. orientation mismatch). Transient CFD simulations can be started from this software within the same workflow, again optimizing interaction time with the system.

The knowledge of a heterogeneous distribution of velocity magnitudes at the aneurysm ostium may be beneficial for optimizing FD treatment: Focal velocity maxima increase the likelihood of remnant inflow jets into the aneurysm. Placing overlapping FD stents could potentially reduce mesh porosity and thus the probability of a remaining inflow jet.

As expected, in all cases, velocity magnitudes inside the aneurysm were reduced after FD treatment, indicating a successful diversion of flow into the aneurysm. Along with this reduction, WSS values also decreased. Changes in pressures were less predictable and varied in magnitude and in once case (case 1), an actual pressure increase was observed. Cebral et al. correlated pressure increase after FD treatment with later aneurysm rupture [10]. An indicator for pressure increase *after* FD treatment from data *before* treatment may therefore be beneficial in evaluating a particular aneurysm for FD placement.

In our study, pressures at the aneurysm ostium before virtual FD

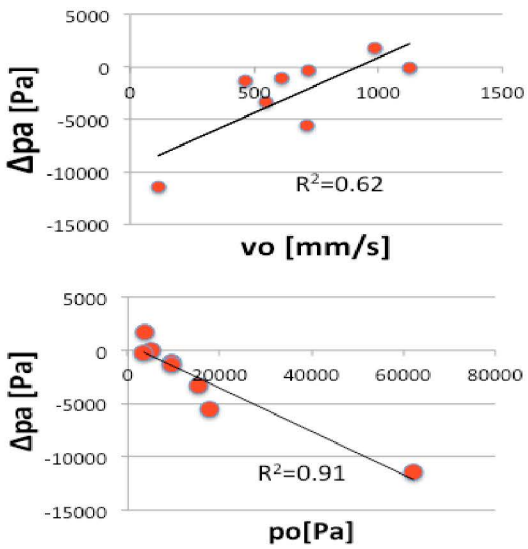

Figure 5: Linear relationship between velocity (vo) and pressure (po) at the ostium site *before* and change in pressure in the aneurysm (Δp_a *) after* virtual FD treatment.

placement correlated with the pressure change inside the aneurysm. Our study has limitations like any CFD study and for a validation of the here presented results, a correlation with actual measurements, such as blood flow velocity magnitudes inside the aneurysm before and after actual FD treatment, as could be obtained by phase contrast magnetic resonance imaging methods, is necessary.

V. Conclusion

Using a dedicated CFD Research Prototype, focal velocity maxima at the aneurysm ostium were visualized and a linear relationship between pressure changes after flow diverter treatment with pressures at the aneurysm ostium site was demonstrated. Further investigations and validation of the here presented simulation results with actual measurement are warranted.

References

[1] L. Pierot, "Flow diverter stents in the treatment of intracranial aneurysms: Where are we?," *J Neuroradiol,* vol. 38, pp. 40-6, Mar.2011

[2] B. Lubicz, L. Collignon, G. Raphaeli, and O. De Witte, "Pipeline flow-diverter stent for endovascular treatment of intracranial aneurysms: preliminary experience in 20 patients with 27 aneurysms," *World Neurosurg,* vol. 76, pp. 114-9, Jul-Aug. 2011

[3] S. Fischer, Z. Vajda, M. Aguilar Perez, E. Schmid, N. Hopf, H. Bazner, and H. Henkes, "Pipeline embolization device (PED) for neurovascular reconstruction: initial experience in the treatment of 101 intracranial aneurysms and dissections," *Neuroradiology,* vol. 54, pp. 369-82, Apr. 2012

[4] J. Raymond, T. E. Darsaut, F. Guilbert, A. Weill, and D. Roy, "Flow diversion in aneurysms trial: the design of the FIAT study," *Interv Neuroradiol,* vol. 17, pp. 147-53, Jun.2011

[5] A. H. Siddiqui, P. Kan, A. A. Abla, L. N. Hopkins, and E. I. Levy, "Complications after treatment with pipeline embolization for giant distal intracranial aneurysms with or without coil embolization," *Neurosurgery,* vol. 71, pp. E509-13; discussion E513, Aug.2012

[6] B. Turowski, S. Macht, Z. Kulcsar, D. Hanggi, and W. Stummer, "Early fatal hemorrhage after endovascular cerebral aneurysm treatment with a flow diverter (SILK-Stent): do we need to rethink our concepts?," *Neuroradiology,* vol. 53, pp. 37-41, Jan. 2011

[7] A. Mantha, C. Karmonik, G. Benndorf, C. Strother, and R. Metcalfe, "Hemodynamics in a cerebral artery before and after the formation of an aneurysm," *AJNR Am J Neuroradiol,* vol. 27, pp. 1113-8, May 2006.

[8] J. R. Cebral, M. A. Castro, J. E. Burgess, R. S. Pergolizzi, M. J. Sheridan, and C. M. Putman, "Characterization of cerebral aneurysms for assessing risk of rupture by using patient-specific computational hemodynamics models," *AJNR Am J Neuroradiol,* vol. 26, pp. 2550-9, Nov-Dec 2005.

[9] L. D. Jou, G. Wong, B. Dispensa, M. T. Lawton, R. T. Higashida, W. L. Young, and D. Saloner, "Correlation between lumenal geometry changes and hemodynamics in fusiform intracranial aneurysms," *AJNR Am J Neuroradiol,* vol. 26, pp. 2357-63, Oct 2005.

[10] J. R. Cebral, F. Mut, M. Raschi, E. Scrivano, R. Ceratto, P. Lylyk, and C. M. Putman, "Aneurysm rupture following treatment with flow-diverting stents: computational hemodynamics analysis of treatment," *AJNR Am J Neuroradiol,* vol. 32, pp. 27-33, Jan. 2011

[11] V. Mihalef, R. Ionasec, P. Sharma, B. Georgescu, I. Voigt, M. Suehling and D. Comaniciu, "Patient-specific modelling of whole heart anatomy, dynamics and haemodynamics from four-dimensional cardiac CT images." *Interface Focus, vol 1, pp. 286-296, Jun 2011*

[12] V. Mihalef, P. Sharma, A. Kamen, and T. Redel, "An immersed porous boundary method for computational fluid dynamics of blood flow in aneurysms with flow diverters", *Proc. ASME Summer Bioengineering Conference, Jun. 2012*